Applied Surface Science 381 (2016) 17–21

Contents lists available at ScienceDirect

Applied Surface Science

journal homepage: www.elsevier.com/locate/apsusc

Photo-induced insulator-metal transition in $Pr_{0.6}Ca_{0.4}MnO_3$ thin films grown by pulsed laser deposition: Effect of thickness dependent structural and transport properties

Tomi Elovaara[a], Hannu Huhtinen[a], Sayani Majumdar[a,b,*], Petriina Paturi[a]

[a] Wihuri Physical Laboratory, Department of Physics and Astronomy, University of Turku, FI-20014 Turku, Finland
[b] Department of Applied Physics, Aalto University School of Science, P.O. Box 15100, FI-00076 Aalto, Finland

ARTICLE INFO

Article history:
Received 11 October 2015
Received in revised form 10 February 2016
Accepted 13 February 2016
Available online 16 February 2016

Keywords:
Insulator-metal transition
Colossal magnetoresistance
Photoinduced effects
Metamagnetic transition
Thin films
Pulsed laser deposition

ABSTRACT

We report photo-induced colossal magnetoresistive insulator-metal transition (IMT) in $Pr_{0.6}Ca_{0.4}MnO_3$ thin films under much reduced applied magnetic field. The colossal effect was studied as a function of film thickness and thus with variable structural properties. Thorough structural, magnetic and magnetotransport characterization under light shows that the highest effect on the transition field can be obtained in the thinnest film (38 nm). However, due to the substrate induced strain of this film the required magnetic field for IMT is quite high. The best crystalline properties of the 110 nm film lead to the lowest IMT field under light and 10^9% change in resistance at 10 K. With increasing thickness, the film properties start to move more toward the bulk material and, hence, IMT is no more observed under the applied field of 9 T. Our results indicate that for obtaining large photo-induced CMR, the best epitaxial quality of thin films is essential.

1. Introduction

Photo-induced insulator-metal (IMT) transition [1,2] in complex metal oxides is a subject of great research interest from both the technological and fundamental point of view. While from the fundamental point of view it opens up a playground for the control of electronic properties using the photonic field [3], from the application point of view this can lead to the orders of magnitude change in electrical resistance under affordable conditions which can be successfully used in logic and memory devices [4]. Colossal magnetoresistive (CMR) manganites, especially the small bandwidth compounds like $Pr_{1-x}Ca_xMnO_3$ (PCMO) (for $0.3 < x < 0.5$) are well-known for their insulator-metallic phase transition under different external factors like the magnetic or electric field, pressure, etc. [5,6]. Under optical excitation this insulator-metal phase transition is further accelerated [7,8]. Recent results confirmed that it is possible to induce IMT at a 50% lower applied magnetic field in the presence of photo-excitation [9]. Now for complex oxide materials, electronic properties are closely correlated with structural properties and effects like substrate induced strain, different crystallinity causing low or high angle grain boundaries, oxygen vacancies, etc. can significantly influence the observed properties [10,11]. In the present work, we have studied the photo-induced IMT in PCMO films with different thicknesses having divergent crystalline properties. As the $SrTiO_3$ (STO) substrate, used to grow the films induces a tensile strain on the PCMO lattice, the thinnest films are expected to be more strained in comparison with the thicker ones. With increasing film thickness the effect of the substrate reduces making the PCMO lattice follow more bulk like properties. In the current studies, we have grown films of four different thicknesses and systematically studied the thin film structural properties using X-ray diffraction, the temperature and field dependent magnetic properties and magneto-transport properties in dark and under light for a comprehensive understanding about the structural change induced effect on photo-induced IMT.

2. Experimental details

PCMO films of four different thicknesses were prepared by pulsed laser deposition on (100) oriented single crystalline STO substrates using a XeCl excimer laser with a pulse wavelength of 308 nm, the pulse duration of 25 ns and a repetition rate of 5 Hz producing a laser fluence of 2 J cm^{-2} on the target. The PCMO target were prepared by the solid state reaction and the details of the

* Corresponding author.
E-mail address: sayani.majumdar@aalto.fi (S. Majumdar).

http://dx.doi.org/10.1016/j.apsusc.2016.02.134
0169-4332/

preparation as well as the structural analysis have been reported elsewhere [13,15]. The flowing oxygen pressure in the chamber was $p = 0.2$ Torr and the substrate temperature during the deposition was 500 °C. In order to achieve the best structural properties as well as the oxygen content of the films, previously optimized in situ post annealing treatments were made at 500 °C in the atmospheric pressure of oxygen with heating and cooling rates of 25 °C min^{-1} [12]. The amounts of laser pulses used were 500, 1500, 3000 and 5000. The thickness (d) was determined using X-ray reflectivity [010] for the thinnest film and was found to be 38 nm. For the thicker films (110 nm, 220 and 360 nm), getting a reflection was impossible and therefore, based on earlier thickness measurements for chemically etched stripes [12], the thicknesses were approximated considering a linear growth [16].

The structural quality of all the samples were investigated using Bruker Innova atomic force microscope and X-ray diffraction measurements made at room temperature using Philips X'Pert Pro diffractometer. The phase purity and crystallinity of the films were confirmed from the θ–2θ scans in out-of-plane (0 b 0) direction and amount of grain boundaries were measured from detailed 2D (φ–2θ) scans of (130) peak to avoid overlapping with the substrate peaks. More information on the structural studies was reported earlier [12]. Magnetization (M) was measured between temperatures 10–300 K with a quantum design superconducting quantum interference device (SQUID) magnetometer with the external magnetic field of 50 mT. Virgin magnetizations as a function of B and magnetic hysteresis curves were recorded between a field of $B = \pm 5$ T at different temperatures between 10–100 K. The external field B was directed always along the planes of the films, i.e., along the PCMO [101] axis. Since the resistivity of the samples is extremely high, the magnetoresistance measurements were performed with PPMS magnetometer using a standard two-point probe with 3.5 mm distance between the contacts and connected to a Keithley 6487 picoammeter. The external field B was always perpendicular to the planes of the films, i.e., along the PCMO [010] axis. The electrical contacts were made to the surface of film with indium brazing. During the magnetoresistivity measurements, the voltage was linearly changed so that the current stays constant at 2 μA between voltages 0.1 and 200 V. The corresponding resistivities are 5×10^4 Ω (0.1 V) and 10^8 Ω (200 V). In the resistivity range below 5×10^4 Ω and over 10^8 Ω, the measuring mode changes to the constant voltage mode where the voltage stays at 0.1 and 200 V, respectively. At the beginning of the magneto-transport measurements, the used voltage is the same for all the samples, inducing the same electric field of 60 kV/m. All the measurements were made in dark and under photoexcitation keeping the other experimental conditions unchanged.

For photo-induced measurements a home-made fiber-optic sample holder attached to the PPMS magnetometer was used where the laser spot covered the entire PCMO surface. An AlGaInP laser diode working at $\lambda = 658$ nm (1.88 eV) was used as the light source with the maximum output power of 10 mW measured at the end of the optical fiber. Hence, the laser fluence on the sample surface was ≈0.4 mW mm^{-2} measured by Thorlabs S120VC photodiode power sensor attached to Thorlabs power meter PM100D. A schematic picture of the measurement setup is presented in Fig. 1.

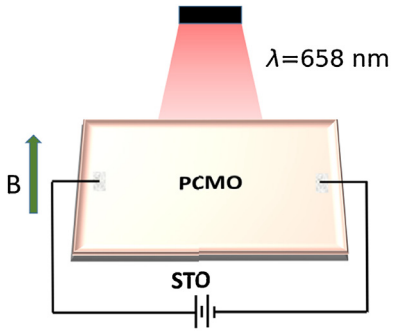

Fig. 1. The schematic representation of the measurement setup.

3. Results and discussion

3.1. Structural properties

From the θ–2θ scans, the peaks corresponding to the out-of-plane lattice parameter (0 b 0) were only observed and this confirms the phase purity of all the deposited samples. From the XRD measurements, the in-plane (a/c) parameters were calculated (the right bottom corner of Fig. 2) and these show that only the thinnest film of 38 nm is under the influence of substrate induced strain, thus stretching the in-plane parameters. In the thicker films, the substrate induced strain is more relaxed and the differences between a/c parameters are within the measurement error. The in-plane lattice parameter values of the thicker films (110–360 nm) matches closely to the bulk PCMO ($x = 0.4$) values [15] justifying our claim. From a closer look of the PCMO (040) peak (Fig. 2), we can clearly see the peak is the highest for the 110 nm thick sample followed by 220 nm, 38 nm and 360 nm samples confirming the best crystalline properties of this sample. The reduction of the peak intensity for the 220 nm and 360 nm films are not consistent with the film thickness. The diffracted intensity should be proportional to the amount of the crystalline material. The θ–2θ scans showed that all the crystallized PCMO material was phase pure and epitaxially textured, but from the intensity-thickness discrepancy we can conclude that not all of the PCMO was well crystallized in the 220 and 360 nm films. This was confirmed from the similar intensity-thickness discrepancy observed in the integrated intensity of (130) φ–2θ peaks. From the φ–2θ scans, the full width at half-maximum (FWHM) in φ-direction was calculated and plotted in the inset of Fig. 2 (the left bottom corner). The result shows with increasing thickness, FWHM first decreases and then starts to increase showing a minimum at 110 nm. The amount of dislocations forming the out-of-plane low angle grain boundaries is comparable to the FHWM φ values and from the above picture we can conclude that it is the smallest in the 110 nm sample. In the thinnest 38 nm film, the broadened FWHM

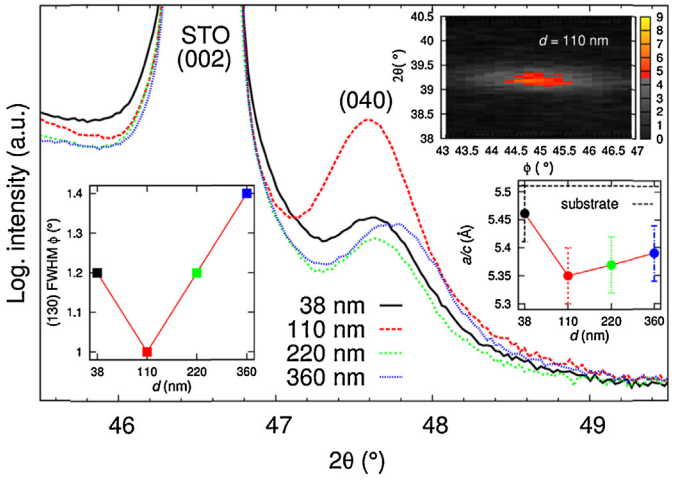

Fig. 2. XRD 2θ diffraction peak (020) of the STO substrate (on the left side) and (040) of the PCMO film (on the right side) for PCMO films of four different thicknesses. (Right top inset) PCMO (130) peak as a function of 2θ and φ for 110 nm film. (Left bottom inset) FWHM in φ-direction calculated from the peak (130) as a function of film thicknesses.